# Connection between the true vibrational density of states and that derived from inelastic neutron scattering

S. N. Taraskin and S. R. Elliott
*Department of Chemistry, University of Cambridge, Lensfield Road, Cambridge CB2 1EW, United Kingdom*
(Received 24 May 1996)

The correction function connecting the true vibrational density of states with that measured in inelastic neutron experiments is defined. Use of this function is essential for multicomponent systems containing elements characterized by rather different scattering lengths or masses. The correction function, calculated for a particular model system (vitreous silica) constructed using molecular dynamics, is shown to be of the order of unity in this case. In the evaluation of the correction function, it has been found that the coherent contribution is negligible and so the incoherent approximation can be successfully applied. The frequency dependence of the correction function arises mainly from that of the partial vibrational density of states. A comparison of the true vibrational density of states with the effective one obtained from an analysis of the dynamical structure factor is presented. [S0163-1829(97)05201-6]

## I. INTRODUCTION

Inelastic neutron scattering is a powerful technique for investigating the dynamical properties of solids and, in particular, atomic vibrations (see, e.g., Ref. 1). One of the basic functions used to characterize atomic dynamics is the vibrational density of states (VDOS). It can be extracted, in principle, from an analysis of the dynamical structure factor $S(\mathbf{Q},\omega)$, which is proportional to the double differential cross section, measured experimentally.[1,2] The difficulty is that the dynamical structure factor is only roughly proportional to the true VDOS especially for the case of multicomponent systems, and several approximations and simplifications have to be made in order to obtain a connection between the VDOS and $S(\mathbf{Q},\omega)$. Generally speaking, it is not always clear, as mentioned in Ref. 2, how good and valid these approximations are and how large is the difference between the true and the effective VDOS. By effective VDOS we mean that obtained from an analysis of the dynamical structure factor. We focus on this question below.

This paper contains a description of the proper way of extracting the true VDOS from inelastic neutron scattering. For that purpose, we have introduced a correction function. This correction function must be calculated in each case for a structural model, e.g., constructed using molecular dynamics (MD). Then the correction function can be used for extracting the true VDOS from the dynamical structure factor, as shown below. The quality of the model structure essentially depends on the interatomic potential implemented in the simulations. For the present purpose, we have chosen the system vitreous silica ($SiO_2$), because, on the one hand, its interatomic potential is well known and, on the other, vitreous silica is of general interest since it can be regarded as being a canonical glass.

The theoretical analysis has been performed in a general form and is valid both for crystalline and noncrystalline condensed atomic structures. The MD simulations, however, were made only for vitreous silica. Different interatomic potentials implemented in the MD simulations result in practically the same correction functions, which shows the universal character of the correction function, at least for the system under consideration.

The structure of this paper is as follows. In Sec. II we define the correction function, connecting the true VDOS and the effective VDOS, obtained from inelastic neutron scattering, and give a simple analytical expression for it. Details of computer simulations are presented in Sec. III. The results of simulations for vitreous silica and a discussion of the behavior of the correction function with variation of different parameters can be found in Sec. IV. Conclusions are given in Sec. V.

## II. BASIC RELATIONS

One of the main characteristics which can be extracted from an analysis of inelastic neutron scattering is the dynamical structure factor $S(\mathbf{Q},\omega)$. For a multicomponent system, it can be written as[1]

$$S(\mathbf{Q},\omega)=\frac{1}{2\pi\hbar N\langle\overline{b^2}\rangle}\int_{-\infty}^{\infty}\sum_{i,i'}\overline{b_i b_{i'}}\langle e^{i\mathbf{Q}\cdot\mathbf{R}_i(0)}e^{i\mathbf{Q}\cdot\mathbf{R}_{i'}(t)}\rangle e^{i\omega t}dt, \tag{1}$$

where $\langle\overline{b^2}\rangle=N^{-1}\Sigma_i\overline{b_i^2}$, with $\overline{b_i}$ the neutron scattering length of atom $i$ ($\overline{b_i}=\overline{b_i}^*$), $N$ the number of atoms in the system (the bar over $b$ means spin and isotope averaging), and $\mathbf{R}_i(t)$ denotes the position of atom $i$ in space at time $t$. For one-phonon processes within the standard harmonic approximation, this expression becomes (see, e.g., Ref. 3)

$$\begin{aligned}S(\mathbf{Q},\omega)=\frac{1}{2N\langle\overline{b^2}\rangle}\sum_{i,i'}\overline{b_i b_{i'}}e^{-W_i(\mathbf{Q})-W_{i'}(\mathbf{Q})}\\ \times\sum_j\frac{(\mathbf{Q}\cdot\mathbf{e}_i^j)(\mathbf{Q}\cdot\mathbf{e}_{i'}^j)}{\sqrt{m_i m_{i'}}\omega_j}(\overline{n_j}+1)e^{i\mathbf{Q}\cdot(\mathbf{R}_{i'}-\mathbf{R}_i)}\\ \times\delta(\omega-\omega_j),\end{aligned} \tag{2}$$

 

where $\mathbf{e}^j(\omega_j)$ are normalized ($\Sigma_i|\mathbf{e}_i^j|^2=1$) $3N$-component eigenvectors (eigenfrequencies) of the dynamical matrix; $m_i$ is the mass of atom $i$ and $\overline{n_j}$ is the thermal-equilibrium occupation number of the vibrational state characterized by frequency $\omega_j$ at temperature $T$,

$$\overline{n_j}=\frac{1}{\exp\{\hbar\omega_j/kT\}-1}, \tag{3}$$

where the bar over $\overline{n_j}$ means thermal-equilibrium averaging. The exponential term in the Debye-Waller factor satisfies the relation

$$W_i(\mathbf{Q})=\frac{1}{2}\langle(\mathbf{Q}\cdot\mathbf{u}_i)^2\rangle=\frac{\hbar Q^2}{2m_i}\sum_j\frac{(\hat{\mathbf{Q}}\cdot\mathbf{e}_i^j)^2}{\omega_j}\left(\overline{n_j}+\frac{1}{2}\right), \tag{4}$$

with $\mathbf{u}_i$ the displacement of atom $i$ and $\hat{\mathbf{Q}}=\mathbf{Q}/Q$.

It is seen from relation (2) that the dynamical structure factor is related to the true VDOS $g(\omega)$ given by

$$g(\omega)=\frac{1}{3N}\sum_{j=1}^{3N}\delta(\omega-\omega_j), \tag{5}$$

so that we can define an effective VDOS as

$$g_{\rm eff}(\mathbf{Q},\omega)=B(Q,\omega)S(\mathbf{Q},\omega). \tag{6}$$

Usually, the function $B(Q,\omega)$ is chosen to be[2]

$$B(Q,\omega)=\frac{2\overline{M}}{\hbar Q^2}e^{2\overline{W}}[\overline{n(\omega)}+1]^{-1}, \tag{7}$$

where $\overline{M^{-1}}=N^{-1}\Sigma_i m_i^{-1}$ and $\overline{W}=N^{-1}\Sigma_i\overline{W}_i$. The Debye-Waller factor in Eq. (7) is averaged over all $\mathbf{Q}$-vector directions separately in $\exp(2\overline{W})$ and $\overline{W}_i$ is expressed by Eq. (4) in which $(\hat{\mathbf{Q}}\cdot\mathbf{e}_i^j)$ is replaced by $|\mathbf{e}_i^j|^2/3$.

We can write the function $B(Q,\omega)$ in a slightly different way, i.e.,

$$B(Q,\omega)=\frac{2\langle\overline{b^2}\rangle}{\hbar Q^2}\frac{\langle m\rangle}{\langle\overline{b^2}e^{-2\overline{W}}\rangle}[\overline{n(\omega)}+1]^{-1}, \tag{8}$$

where $\langle m\rangle=N^{-1}\Sigma_i m_i$ and $\langle\overline{b^2}e^{-2\overline{W}}\rangle=N^{-1}\Sigma_i\overline{b_i^2}e^{-2\overline{W}_i}$. Such a choice of $B(Q,\omega)$ results in the coincidence of the effective and true VDOS for the zero-frequency modes characterizing the displacement of a sample as a whole (see also below).

The dynamical structure factor $S(\mathbf{Q},\omega)$ in Eq. (6) can be obtained from an analysis of inelastic neutron scattering data, while the average Debye-Waller factor in Eqs. (7) and (8) is available from a comparison of the $Q$ dependence of the elastic line for neutron scattering with diffraction data.[2] Therefore the effective VDOS is an experimentally measurable function. The problem is that it is related to the true VDOS via the correction function $C(\mathbf{Q},\omega)$, defined by the relation

$$g_{\rm eff}(\mathbf{Q},\omega)=C(\mathbf{Q},\omega)g(\omega)=\frac{1}{3N}\sum_j^{3N}C(\mathbf{Q},\omega_j)\delta(\omega-\omega_j), \tag{9}$$

and $C(\mathbf{Q},\omega)$ is not necessarily close to unity.

The effective VDOS depends not only on frequency but on $\mathbf{Q}$ as well. The standard way of avoiding this dependence is to average $g_{\rm eff}(\mathbf{Q},\omega)$ over $\mathbf{Q}$ vectors in a definite range of $Q$:[2]

$$\overline{g_{\rm eff}}(\omega)=\frac{1}{Q_2-Q_1}\int_{Q_1}^{Q_2}\langle g_{\rm eff}(\mathbf{Q},\omega)\rangle_{\mathbf{\Omega}}dQ, \tag{10}$$

with

$$\langle g_{\rm eff}(\mathbf{Q},\omega)\rangle_{\mathbf{\Omega}}=\int_{\mathbf{\Omega}}g_{\rm eff}(\mathbf{Q},\omega)d\mathbf{\Omega}, \tag{11}$$

where the angular brackets denote the averaging over $\mathbf{Q}$-vector directions and $\mathbf{\Omega}$ is the solid angle. In the case of systems of finite size that are used in computer simulations, only a restricted set of wave vectors is available, i.e.,

$$\mathbf{Q}=\left\{\frac{2\pi}{L_x}n_x,\ \frac{2\pi}{L_y}n_y,\ \frac{2\pi}{L_z}n_z\right\},$$

where $L_\alpha$ are the box side lengths and $n_\alpha$ are integer numbers. Averaging over $\mathbf{Q}$ in this case can be done as

$$g_{\rm eff}(\omega)=\frac{1}{N_Q}\sum_{\mathbf{Q}}g_{\rm eff}(\mathbf{Q},\omega). \tag{12}$$

Here the sum is taken over all available $\mathbf{Q}$ or $Q$ belonging to a particular range, and $N_Q$ stands for the number of terms in the sum. This simple averaging gives a slightly different result to that arising from Eqs. (10) and (11), but seems to be closer to the procedure used in experimental neutron scattering data processing.

Substituting $C(\mathbf{Q},\omega)$ from the definition (9) in Eqs. (10) and (11) one can obtain similar expressions for the averaged correction function

$$\overline{C}(\omega)=\frac{1}{Q_2-Q_1}\int_{Q_1}^{Q_2}\langle C(\mathbf{Q},\omega)\rangle_{\mathbf{\Omega}}dQ \tag{13}$$

or

$$C(\omega)=\frac{1}{N_Q}\sum_{\mathbf{Q}}C(\mathbf{Q},\omega), \tag{14}$$

so that

$$g_{\rm eff}(\omega)=C(\omega)g(\omega). \tag{15}$$

To extract the main contribution to $C(\omega)$ when averaging over $\mathbf{Q}$ it is convenient to separate the coherent and incoherent parts in $C(\mathbf{Q},\omega)$, bearing in mind Eqs. (2), (6), and (9):

$$C(\mathbf{Q},\omega_j)=C_{\rm incoh}(\mathbf{Q},\omega_j)+C_{\rm coh}(\mathbf{Q},\omega_j), \tag{16}$$

where

$$C_{\rm incoh}(\mathbf{Q},\omega_j)=A\sum_i\frac{\overline{b_i^2}}{m_i}e^{-2\overline{W_i}(Q)}(\hat{\mathbf{Q}}\cdot\mathbf{e}_i^j)^2 \tag{17}$$

and

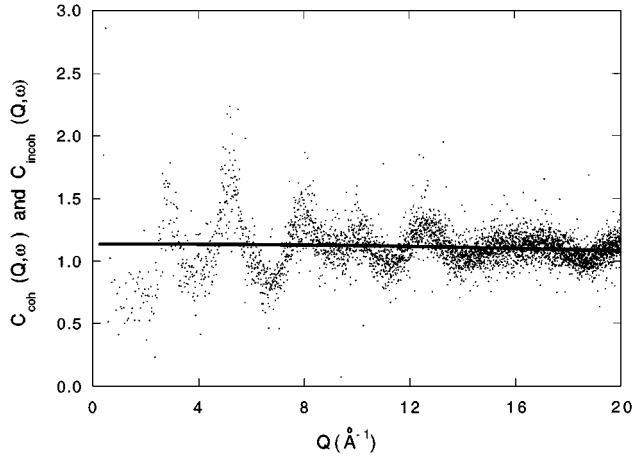


FIG. 1. Coherent (dots) and incoherent (solid line) contributions to the correction function calculated for a model of vitreous silica at a frequency $\nu=\omega/2\pi=3.02$ THz and temperature $T=50$ K.

$$C_{\rm coh}(\mathbf{Q},\omega_j)=A\sum_{i\neq i'}\frac{\overline{b_i}\,\overline{b_{i'}}}{\sqrt{m_i m_{i'}}}e^{-\overline{W_i}(Q)-\overline{W_{i'}}(Q)}(\hat{\mathbf{Q}}\cdot\mathbf{e}_i^j)\times(\hat{\mathbf{Q}}\cdot\mathbf{e}_{i'}^j)e^{i\mathbf{Q}\cdot(\mathbf{R}_{i'}-\mathbf{R}_i)}, \tag{18}$$

with

$$A=\frac{3\langle m\rangle}{\langle\overline{b^2}e^{-2\overline{W}}\rangle}. \tag{19}$$

Here we have used the definition (9) of the correction function and the connection (6) of the effective VDOS to the dynamical structure factor (2) via the function $B(Q,\omega)$ defined in Eq. (8).

For isotropic systems, an analytical averaging over $\mathbf{Q}$ directions can be done, resulting in the following expression:

$$\begin{aligned}C(Q,\omega_j)&=\langle C_{\rm incoh}(\mathbf{Q},\omega_j)+C_{\rm coh}(\mathbf{Q},\omega_j)\rangle_{\mathbf{\Omega}}\\&=C_{\rm incoh}(Q,\omega_j)+C_{\rm coh}(Q,\omega_j)\\&=\frac{A}{3}\sum_i\frac{\overline{b_i^2}}{m_i}e^{-2\overline{W}_i(Q)}|\mathbf{e}_i^j|^2\\&\quad+A\sum_{i\neq i'}\frac{\overline{b_i}\,\overline{b_{i'}}}{\sqrt{m_i m_{i'}}}e^{-\overline{W_i}(Q)-\overline{W_{i'}}(Q)}F_{ii'}(Q),\end{aligned} \tag{20}$$

where the function $F_{ii'}(Q)$ is given by[4]

$$F_{ii'}(Q)=\frac{(\mathbf{R}_{ii'}\cdot\mathbf{e}_i^j)(\mathbf{R}_{ii'}\cdot\mathbf{e}_{i'}^j)}{R_{ii'}^4}\left(3\cos q+q\sin q-3\frac{\sin q}{q}\right)+\frac{(\mathbf{e}_i^j\cdot\mathbf{e}_{i'}^j)}{R_{ii'}^2}\left(\frac{\sin q}{q}-\cos q\right), \tag{21}$$

with $\mathbf{R}_{ii'}=\mathbf{R}_{i'}-\mathbf{R}_i$ and $q\equiv QR_{ii'}$. The incoherent part of Eq. (20) is practically independent of $Q$ because this dependence is only due to a slight monotonic variation of the Debye-Waller factor with $Q$ [see Eq. (4)]. The coherent part, on the other hand, oscillates strongly with $Q$ (see Fig. 1). However, these oscillations mainly cancel each other out when averaging over $Q$ (as also follows from our numerical analysis; see Fig. 5), so that only the incoherent part makes the major contribution to the integral (13) or the sum (14). In

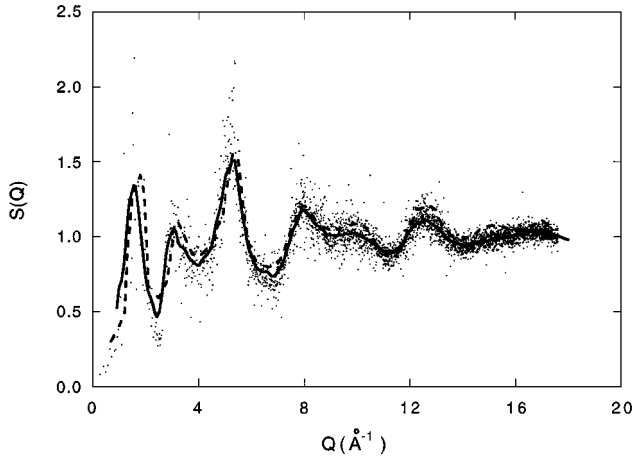


FIG. 2. Static structure factor for vitreous silica: dots, numerical averaging over available $\mathbf{Q}$ vectors; solid line, analytical averaging over $\mathbf{Q}$ directions; dashed line, experimental data (Ref. 12).

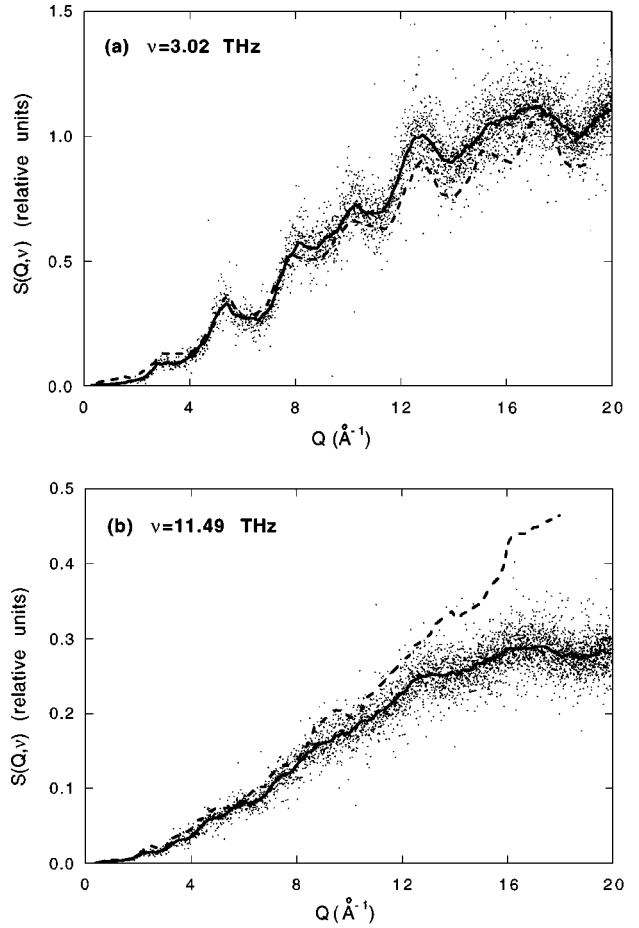


FIG. 3. Dependence of the dynamical structure factor $S(Q,\nu)$ on $Q$ for vitreous silica at two different frequencies for which comparison with experiment (Ref. 12) is available: (a) $\nu_1=3.02$ THz and (b) $\nu_2=11.49$ THz (the same notations as in Fig. 2). The same scaling factor for the dynamical structure factor was used at both frequencies.

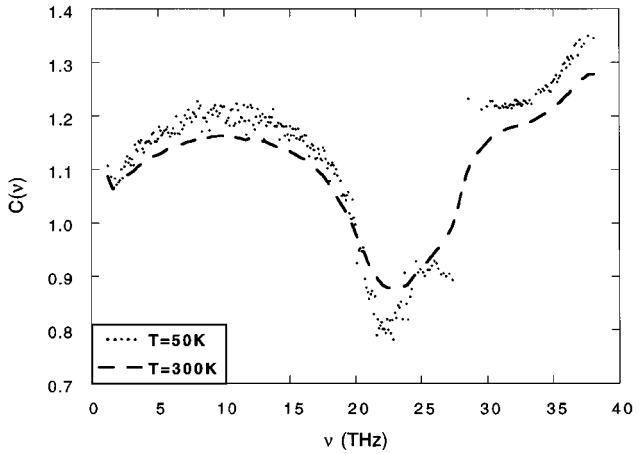


FIG. 4. Frequency dependence of the calculated correction function for vitreous silica at two temperatures. The dashed line represents smoothed data at $T=300$ K.

the incoherent approximation, which is often used for $g_{\rm eff}(\omega)$,[2] $C(Q,\omega_j)\simeq C_{\rm incoh}(Q,\omega_j)$ and expression (20) can be rewritten as

$$C(Q,\omega_j)\simeq\frac{A}{3}\sum_\alpha\frac{\overline{b_\alpha^2}}{m_\alpha}e^{-2\overline{W}_\alpha(Q)}\rho_\alpha(\omega_j),\tag{22}$$

with $\alpha$ running over all species of atoms in the system. Here $\rho_\alpha(\omega_j)$ is the relative partial VDOS for atoms of type $\alpha$, i.e.,

$$\rho_\alpha(\omega_j)=\frac{g_\alpha(\omega_j)}{g(\omega_j)}=\sum_{i\ni\alpha}|\mathbf{e}_i^j|^2,\tag{23}$$

where $i$ signifies all atoms of type $\alpha$. An important property of the correction function written in this way is that it is equal to unity for the zero-frequency mode (the rigid-body displacement). Indeed, for the zero-frequency mode the sample is displaced as a whole, so that the displacements of different atoms $|\mathbf{u}_i|\sim|\mathbf{e}_i^{(j=0)}|/\sqrt{m_i}$ are equal to each other, resulting in the following atomic components of the normalized eigenvector

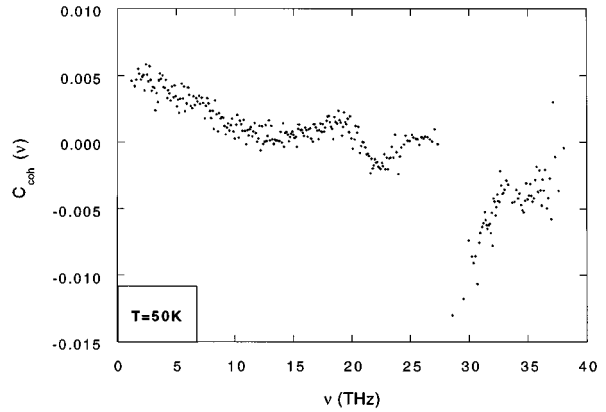


FIG. 5. Coherent contribution to the correction function for vitreous silica.

$$|\mathbf{e}_{i=\alpha}^{(j=0)}|=\frac{\sqrt{m_\alpha}}{\Sigma_{i'=1}^N m_{i'}}\tag{24}$$

for atoms of type $\alpha$. Then, the zero-frequency partial VDOS $\rho_\alpha^{(0)}\equiv\rho_\alpha(0)$, as follows from Eq. (23), obviously satisfies the relation

$$\rho_\alpha^{(0)}=\frac{\Sigma_{i\ni\alpha}m_i}{\Sigma_{i=1}^N m_i}=\frac{N_\alpha m_\alpha}{\Sigma_{\alpha'}N_{\alpha'}m_{\alpha'}}=\frac{N_\alpha m_\alpha}{N\langle m\rangle}.\tag{25}$$

Substituting this expression in Eq. (22) and bearing in mind the definition (19) one can easily see that $C(Q,\omega=0)\simeq 1$. This property allows us to rewrite Eq. (22) in the following more convenient form

$$\begin{aligned}C(Q,\omega_j)&\simeq 1+\frac{A}{3}\sum_\alpha\frac{\overline{b_\alpha^2}}{m_\alpha}e^{-2\overline{W}_\alpha(Q)}[\rho_\alpha(\omega_j)-\rho_\alpha^{(0)}]\\&\equiv 1+\delta C(Q,\omega_j)\end{aligned}\tag{26}$$

to separate the deviation $\delta C(Q,\omega_j)$ of the correction function from unity. It should be noted that the equality $C(Q,\omega=0)\simeq 1$ is based on the proper choice of the normalization constant (19) following from the definition (8).

A further simplification in the expression (26) can be made by putting the Debye-Waller factors equal to unity,

$$e^{-2\overline{W}_\alpha(Q)}=e^{-Q^2\langle u_\alpha^2\rangle/3}\simeq 1,\tag{27}$$

which is valid for $Q^2\langle u_\alpha^2\rangle/3\ll 1$, with $\langle u_\alpha^2\rangle$ being the mean square atomic displacement. For vitreous silica, as follows from our simulations, $\langle u_{\rm ox}^2\rangle\simeq 0.00\,17$ Å$^2$ and $\langle u_{\rm si}^2\rangle\simeq 0.000\,96$ Å$^2$ at $T=50$ K and therefore approximation (27) is relevant for $Q\lesssim 17$ Å$^{-1}$. If relation (27) is fulfilled, then the correction function (26) reduces to

$$C(\omega)\simeq 1+\frac{A}{3}\sum_\alpha\frac{\overline{b_\alpha^2}}{m_\alpha}[\rho_\alpha(\omega)-\rho_\alpha^{(0)}],\tag{28}$$

which depends now only on frequency.

If the correction function equals unity, then $g_{\rm eff}(\omega)$ obviously coincides with the true VDOS. This is the case when the partial density of states does not depend on frequency and is equal to the zero-frequency value $\rho_\alpha^{(0)}$. However, in reality the situation is quite different and $\delta C\neq 0$. The behavior of $\delta C(\omega)$ is mainly due to the frequency dependence of the partial VDOS or, to be more exact, to $[\rho_\alpha(\omega)-\rho_\alpha^{(0)}]\sim 1$. The value of $\delta C$ also depends on the relative masses and the relative neutron scattering lengths of atoms of different types. To estimate the minimum and maximum values that the correction function can take, let us consider the simplest case, namely, a two-component system, $\alpha=1,2$. In this case, expression (28) can be rewritten as

$$C(\omega)=1+\frac{A}{3}[\rho_1(\omega)-\rho_1^{(0)}]\left(\frac{\overline{b_1^2}}{m_1}-\frac{\overline{b_2^2}}{m_2}\right).\tag{29}$$

Here we took into account the relation

$$\rho_2(\omega)-\rho_2^{(0)}=-[\rho_1(\omega)-\rho_1^{(0)}],\tag{30}$$

following from the normalization of the relative partial VDOS: $\rho(\omega)=\rho_1(\omega)+\rho_2(\omega)=1$. Let us suppose, for definiteness, that $\overline{b_1^2}/m_1>\overline{b_2^2}/m_2$. Then, the minimum and maximum values of the correction function can be easily estimated from Eq. (29):

$$C(\omega)\gtrsim C_{\min}=C(\omega)\big|_{\rho_1(\omega)=0}\simeq\frac{\overline{b_2^2}\langle m\rangle}{m_2\langle\overline{b^2}\rangle}, \tag{31}$$

while the maximum value is

$$C(\omega)\lesssim C_{\max}=C(\omega)\big|_{\rho_1(\omega)=1}\simeq\frac{\overline{b_1^2}\langle m\rangle}{m_1\langle\overline{b^2}\rangle}. \tag{32}$$

From Eqs. (31) and (32), it follows that the deviation of the correction function from unity is determined by the relative mass $m_\alpha/\langle m\rangle$ and the relative neutron scattering cross section $\overline{b_\alpha^2}/\langle\overline{b^2}\rangle$. For the majority of multicomponent systems, these quantities are of the order of unity, i.e., $\delta C\lesssim 1$, e.g., for vitreous silica $C_{\min}=0.58$ and $C_{\max}=1.48$ (cf. the range of variation of the correction function calculated for vitreous silica in Fig. 4). However, for compounds containing elements characterized by very different scattering lengths or masses, the correction function can deviate appreciably from unity, e.g., $C_{\min}=0.18$ and $C_{\max}=2.59$ for AlN.

It should be noted that the effective VDOS defined in Eqs. (9)–(12) is not normalized by unity. Indeed, as follows from Eqs. (9), (12), and (14),

$$G=\int_0^\infty g_{\text{eff}}(\omega)\,d\omega=\frac{1}{3N}\sum_j C(\omega_j). \tag{33}$$

In the incoherent approximation (22), the normalization constant $G$ can be easily calculated, using the normalization property of eigenvectors ($\Sigma_j|\mathbf{e}_i^j|^2=3$, with the summation over frequencies) and neglecting the Debye-Waller factors being close to unity,

$$G=\sum_j C(\omega_j)=\frac{A}{3N}\sum_i\frac{\overline{b_i^2}}{m_i}\equiv\frac{\langle m\rangle\langle\overline{b^2}/m\rangle}{\langle\overline{b^2}\rangle}. \tag{34}$$

For most substances the value of $G$ is close to unity; e.g., for vitreous silica $G=1.14$.

The above analysis has been performed in a general form and is valid both for crystalline and noncrystalline condensed atomic structures. The MD simulations described below, however, were made only for vitreous silica. Different interatomic potentials, implemented in the MD simulations, result in practically the same correction functions, thus showing the universal character of the correction function, at least for the system under consideration.

## III. DETAILS OF SIMULATIONS

The analysis of the VDOS described in the previous section was performed numerically for a particular system, vitreous silica. Several models of vitreous silica containing 648 atoms were constructed using the molecular dynamics package DLPOLY (Ref. 5) (NVE ensemble, periodic boundary conditions, Ewald summation for Coulombic interactions). Different atomic potentials were implemented, namely, the Tsuneyuki[6] and Van Beest[7] potentials. At small interatomic distances, these potentials have an energy barrier. However, the energy barrier is not high enough to prevent atoms at high temperatures from hopping over it and becoming coincident. We have therefore used the modified Tsuneyuki and Van Beest potentials,[8] which are free of this fault due to the inclusion of an increased energy barrier at small interatomic separations.

The systems were quenched from the liquid state at 5000 K, decreasing the temperature by 100 K steps. At every fixed temperature, a MD run of $\sim$60 ps was made to equilibrate the system by velocity rescaling every $10^{-2}$ ps. The time step was chosen to be $10^{-3}$ ps, being significantly smaller than the smallest vibrational time in silica, $\tau_{\min}\sim 1/\nu_{\max}$ $\sim$1/40 THz $\sim 2.5\times 10^{-2}$ ps. The quench continued until the temperature was reached at which atomic diffusion stopped. For the Van Beest potential, the diffusion stopped (for a run lasting for $t\lesssim 10^2$ ps) at $T\simeq 2500$ K, while for the Tsuneyuki potential the corresponding temperature was $\sim$2000 K. Then a zero-temperature energy minimization, implemented in DLPOLY, was performed on the models. The systems reached their metastable ''glass'' minima and the fact that the system really was in the energy minimum was checked by both conjugate and steepest-descent methods. The dynamical matrix for the relaxed system was calculated and diagonalized directly, giving the eigenvectors $\{\mathbf{e}^j\}$ and eigenvalues $(\omega_j)$.

## IV. RESULTS AND DISCUSSION

All the models of vitreous silica that we have studied show similar vibrational properties. Both the Tsuneyuki[6] and the Van Beest[7] potentials used in the MD simulations are based on *ab initio* calculations of small molecular clusters, but the high-frequency edge of the vibrational spectrum of the Tsuneyuki system is shifted to lower frequencies by $\sim$5 THz (Ref. 9), while the vibrational spectrum of the Van Beest system coincides with experiment much better.[10] We have also investigated the vibrational properties of a model of vitreous silica created with the three-body empirical Feuston-Garofalini potential.[11] Unlike the two above-mentioned systems, the Feuston-Garofalini structure contains a few coordination defects and gives relatively poor agreement with the experimental dynamical structure factor. Therefore the Van Beest potential seemed to give the best results overall (all figures reported here represent the numerical data calculated for a vitreous silica model constructed with the Van Beest potential), and the resulting structure gave very good agreement with experimental neutron-scattering data (see Figs. 2 and 3).

Figure 2 shows the dependence of the static structure factor $S(Q)$ on the magnitude of the wave vector for both simulated and experimental data. The computational results are based on the following general expression for the static structure factor $S(\mathbf{Q})$:[1]

$$S(\mathbf{Q})=1+\frac{1}{N\langle\overline{b^2}\rangle}\sum_{i\neq i'}\overline{b_i}\;\overline{b_{i'}}\,e^{-W_{ii'}}e^{i\mathbf{Q}\cdot(\mathbf{R}_i-\mathbf{R}_{i'})}, \tag{35}$$

with

$$W_{ii'} = \frac{\hbar Q^2}{6} \sum_j \left( \frac{\mathbf{e}_i^j}{\sqrt{m_i}} - \frac{\mathbf{e}_{i'}^j}{\sqrt{m_{i'}}} \right)^2 \frac{\overline{n_j} + 1/2}{\omega_j}. \quad (36)$$

For isotropic systems, analytical averaging over all **Q** directions gives the Debye expression

$$S(Q) = \langle S(\mathbf{Q}) \rangle_{\mathbf{\Omega}} = 1 + \frac{1}{N \langle \overline{b^2} \rangle} \sum_{i \neq i'} \overline{b_i b_{i'}} e^{-W_{ii'}} \frac{\sin Q|\mathbf{R}_i - \mathbf{R}_{i'}|}{Q|\mathbf{R}_i - \mathbf{R}_{i'}|}. \quad (37)$$

The results obtained from Eq. (37) for our system are indicated by the solid curve in Fig. 2, and the dots represent the result of simple (arithmetic) averaging, according to relation (35), over all available **Q** vectors with a fixed magnitude of $Q$. The dashed curve represents the experimental data.[12] As shown in Fig. 2, the simulated static structure factor fits the experimental curve reasonably well. A slight deviation appears, however, at $Q \gtrsim 15$ Å$^{-1}$, where the experimental data could be less reliable.

Figure 3 gives a comparison of simulated and experimental data[12] for the dynamical structure factor at two fixed frequencies $\nu_1 = 3.02$ THz and $\nu_2 = 11.49$ THz. The experimental curve for the frequency $\nu_1$ has a very pronounced structure and all its peaks (except for $Q \gtrsim 15$ Å$^{-1}$, as mentioned above) are well reproduced in our calculations. The dots in Fig. 3, as in Fig. 2, are obtained by directional averaging over all **Q** vectors with fixed $Q$, while the solid line results from an analytical averaging over all directions at fixed $Q$. At the higher frequency $\nu_2$, the dynamical structure factor has less pronounced features, but again the calculated data fit the experimental curve rather well.

The agreement between the calculated and measured static and dynamical structure factors demonstrates the high quality of the model of the vitreous silica system under consideration.

The goal of our analysis is the correction function $C(\omega)$. We can easily calculate it knowing the eigenvectors and eigenvalues of the dynamical matrix of the silica structure in question. The calculated frequency dependence of the correction function at two different temperatures is illustrated in Fig. 4. The calculations were made according to expression (14) in which averaging over $Q$ was performed in the range 6 Å$^{-1} \lesssim Q \lesssim 13$ Å$^{-1}$. This correction function is mainly due to the incoherent contribution in Eq. (20). The coherent contribution to the correction function is shown in Fig. 5. It is practically independent of temperature and is two orders of magnitude smaller than the incoherent part. This is due to the fluctuations of $C_{\mathrm{coh}}(Q,\omega)$ with $Q$ which cancel each other out on averaging over $Q$. The negligible contribution of the coherent part to the correction function confirms the validity of the incoherent approximation, at least for silica (see Ref. 2).

The shape of the correction function results mainly from the frequency dependence of the oxygen-based partial VDOS, namely, $\sim[\rho_{\mathrm{ox}}(\omega) - \rho_{\mathrm{ox}}^{(0)}]$, as follows from Eq. (22): $(\overline{b_{\mathrm{ox}}^2}/m_{\mathrm{ox}} > \overline{b_{\mathrm{si}}^2}/m_{\mathrm{si}}$ for silica). The frequency dependence of $[\rho_{\mathrm{ox}}(\omega) - \rho_{\mathrm{ox}}^{(0)}]$ is presented in Fig. 6, which clearly shows that the shape of this function is reproduced in the correction function (see Fig. 4).

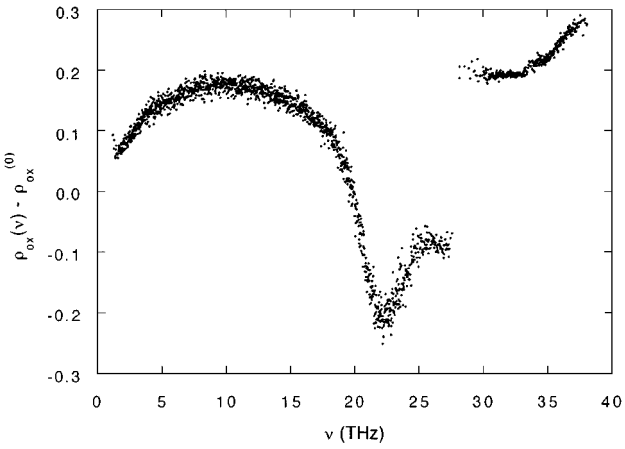


FIG. 6. The calculated partial vibrational density of states for oxygen atoms in a model of vitreous silica.

The temperature dependence of the correction function is mainly due to the Debye-Waller factor. At higher temperatures, the average mean square atomic displacement $\langle u^2 \rangle$ increases, and the Debye-Waller factor correspondingly decreases, since $\exp(\overline{W}) \sim \exp\{-Q^2 \langle u^2 \rangle / 6\}$. This leads to the decrease of the correction function deviation $\delta C$ from unity at higher temperatures (see Fig. 4).

It should be noted that the correction function depends only slightly on the range of $Q$ over which the averaging is performed. The change in the calculated value of $C(\omega)$ is only about a few percent when the averaging over $Q$ is made instead in the range 0.3 Å$^{-1} \lesssim Q \lesssim 19$ Å$^{-1}$.

According to the definition (15), the correction function can be used to obtain the true VDOS from an effective neutron-derived VDOS, as demonstrated in Fig. 7. Here the experimental data (triangles) (Ref. 13) have to be compared with the dotted line related to the effective VDOS obtained from the computer simulations. To make a proper comparison between these two curves, we normalized the integrated area of the experimental VDOS by the constant $G$, as defined in Eq. (33), because the area under the dashed line is normalized as well by the same value of $G$ [see Eqs. (33) and

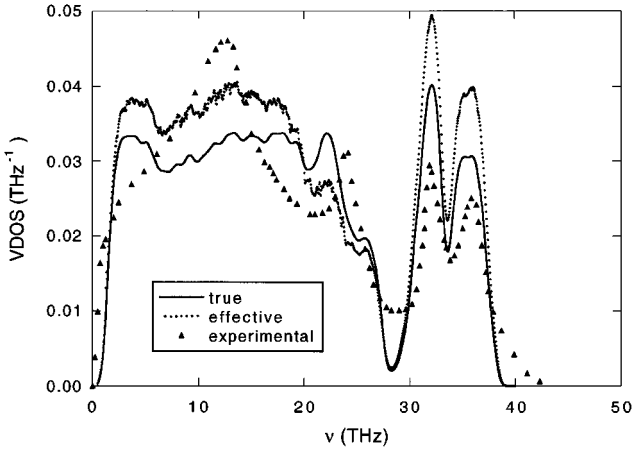


FIG. 7. True (solid line), effective (dotted line), and experimental (triangles) (Ref. 13) vibrational densities of states for vitreous silica, the former two obtained from computer simulations.

(34)]. The effective VDOS mainly follows the true one (solid line), because the correction function is of the order of unity. However, some specific features in the true VDOS could not be reproduced by the effective VDOS, e.g., low-frequency peculiarities such as the boson peak. Our calculated results in this frequency region are not sufficiently reliable because of the finite size of the system (similar simulations with larger systems are in progress).

The main purpose of our analysis has been to show how properly to extract the true VDOS from inelastic neutron scattering data. Based on the considerations presented above, we propose the following way to do this. First, the dynamical structure factor is to be calculated. Then the effective VDOS in accordance with definitions (5) and (8) should be calculated and averaged over **Q**-vector directions. Next, the correction function has to be found, e.g., from a vibrational analysis of a model structure constructed by using, for example, molecular dynamics. The last step involves the multiplication of the effective VDOS by the correction function, resulting in the true VDOS.

## V. CONCLUSIONS

We have defined the correction function for the relative difference between the true vibrational density of states and that obtained from an analysis of inelastic neutron scattering experiments. The incoherent approximation is relevant in the correction function evaluation, and the frequency dependence of the correction function is mainly due to that of the partial vibrational density of states (projected on a particular atom type). The magnitude of the correction function for multicomponent systems depends on the relative masses and scattering lengths and appears to be of the order of unity for the majority of substances. This means that the effective vibrational density of states measured in inelastic neutron scattering experiments generally fits the true density of states sufficiently well. This correction function was calculated for a particular system—vitreous silica—and appeared to differ from unity by not more than 20% in that case.

We think that this correction function will be very useful in obtaining vibrational densities of states from analyses of inelastic neutron scattering data. It can be calculated for model structures, e.g., constructed using molecular dynamics, and then used for processing the experimental data.

## ACKNOWLEDGMENTS

We would like to thank the authors of Ref. 8 for sending us a copy of their work prior to publication. One of the authors (S.N.T.) is grateful to Trinity College, Cambridge (UK) for financial support.

[1] D.L. Price, and K. Sköld, in *Neutron Scattering*, edited by K. Sköld and D.L. Price (Academic, London, 1986), Pt. A.
[2] D.L. Price and J.M. Carpenter, J. Non-Cryst. Solids **92**, 153 (1987).
[3] S.W. Lovesey, *Theory of Neutron Scattering from Condensed Matter* (Clarendon Press, Oxford, 1986).
[4] J.M. Carpenter and C.A. Pelizzari, Phys. Rev. B **12**, 2391 (1975).
[5] W. Smith and T.R. Forester, J. Mol. Graphics (to be published).
[6] S. Tsuneyuki, M. Tsukada, H. Aoki, and Y. Matsui, Phys. Rev. Lett. **61**, 869 (1988).
[7] B.W.H. Van Beest, G.J. Kramer, and R.A. Van Santen, Phys. Rev. Lett. **64**, 1955 (1990).
[8] Y.Guissani and B. Guillot, J. Chem. Phys. **104**, 7633 (1996).
[9] R.G. Della Valle and E. Venuti, Chem. Phys. **179**, 411 (1994).
[10] C.J. Kramer, N.P. Farragher, B.W.H. Van Beest, and R.A. Van Santen, Phys. Rev. B **43**, 5068 (1991).
[11] B. Feuston and S.H. Garofalini, J. Chem. Phys. **89**, 5818 (1988).
[12] A.C. Hannon, M. Arai, R.N. Sinclair, and A.C. Wright, J. Non-Cryst. Solids **150**, 239 (1992).
[13] M. Arai, A.C. Hannon, A.D. Taylor, T. Otomo, A.C. Wright, R.N. Sinclair, and D.L. Price, Trans. Am. Crystallogr. Assoc. **27**, 113 (1991).